Results in Physics 7 (2017) 2705–2710

Contents lists available at ScienceDirect

Results in Physics

journal homepage: www.journals.elsevier.com/results-in-physics

Urban UV environment in a sub-tropical megacity – A measurement and modelling study

Ka-Ming Wai [a,b,*], Peter K.N. Yu [a,*], Pok-Man Chan [a]

[a] Department of Physics and Materials Science, City University of Hong Kong, Hong Kong Special Administrative Region
[b] Institute of Future Cities, Chinese University of Hong Kong, Hong Kong Special Administrative Region [1]

ARTICLE INFO

Article history:
Received 28 March 2017
Received in revised form 21 July 2017
Accepted 24 July 2017
Available online 28 July 2017

ABSTRACT

The variations of solar total UV (UVA + UVB) exposure rates in a megacity featured with high-rise buildings during summer months were measured and relevant model predictions were evaluated. The maximum pedestrian-level total solar UV exposure rate was less than the un-obstructed exposure rate at any time, attributing to the prevailing reduction in the diffuse solar radiation due to the obstruction effects of distant buildings. Comparing with the measurements, our coupled model well captured the spatial and temporal variations of the reduction of UV exposure rates. By measurements, large reduction in the solar total UV exposure rate down to 12% of un-obstructed exposure rate due to the building obstruction effects was found, agreeing with our previous simulation results and results from an Australian megacity. On the other hand, building reflection from reflective curtain walls could reach 23% of the un-obstructed solar total UV exposure rate at the ground level. This implied improper building design creating additional harmful effects of solar UV radiation on the environment. The coupled model was also applied to predict the urban UV exposure rates during a tropical-cyclone induced aerosol episode. A well-evaluated urban solar UV model is an important tool for sustainable urban design.

Introduction

Most solar UV-C (100–280 nm) radiation is absorbed by the stratospheric ozone layer, leaving only UV-A (315–400 nm) and a small amount of UV-B (280–315 nm) radiation to penetrate the atmosphere and reach the earth surface. Solar UV radiation can be beneficial for the lives on earth, for example, UVB radiation is essential for vitamin D production [1–3]. Vitamin D production from UVB exposure is also related to body orientation [4]. On the other hand, solar UV radiation is also related to numerous health hazards. The UVA radiation causes immunosuppression [5], skin aging [6] and melanoma [7]. Harmful effects of the UVB radiation include sunburn, skin cancer and eye damage [1].

The UV radiation on the Earth's surface had been extensively studied in open areas [8–10], but relevant measurements or modelling studies in megacities with skyscrapers were rarely found in the literature. The UV distribution in the urban building environment is highly complicated, which consists of a combination of areas with UV attenuation in building shadows, "hotspots" at ground level due to solar reflection (or glare) from curtain walls of skyscrapers and unobstructed solar irradiation. As such, humans at the ground level frequently receive different UV exposure rates as compared to open areas. Recently, the measurements by McKinley et al. [11] indicated that there was four times less of vitamin D produced within the urban environment. Soontrapa et al. [12] reported a higher risk of vitamin D deficiency for volunteers in the study living in urban area relative to those living in suburban area in Thailand. Goswami et al. [13] also had similar finding in northern India. Moreover, Hong Kong is influenced by continental outflow of high aerosol loadings under certain meteorological conditions [14,15] (i.e., the nearby tropical cyclone in the current study), but the modification of the abovementioned UV distribution due to aerosol effects such as scattering has rarely been studied.

Spectro-radiometers, broad-band radiometers and total UV meters [8,9,16,17] are typical instruments to measure solar UV radiation. Recently, Butson et al. [18] and Chun and Yu [17] develop passive, less expensive radiochromic film detector to measure the UV radiation. For computer simulations, radiative transfer models were used to estimate the UV radiation levels in open areas, taking into consideration the solar azimuth angle, atmospheric column ozone, presence of clouds and atmospheric aerosol

* Corresponding authors at: Department of Physics and Materials Science, City University of Hong Kong, Hong Kong Special Administrative Region (K.-M. Wai and P.K.N. Yu).
E-mail addresses: bhkmwai@cityu.edu.hk (K.-M. Wai), peter.yu@cityu.edu.hk (P.K.N. Yu).
[1] Now in.

http://dx.doi.org/10.1016/j.rinp.2017.07.055
2211-3797/

concentrations [19,20]. However, a model which is applicable to high-density urban area is absent.

In view of the above, the objectives of our study were to investigate the effects of high-rise buildings on the surface- (or pedestrian-) level urban UV environment of Hong Kong during the clear-sky condition and an aerosol episode by measurements, and evaluate the performance of a "coupled model" which is described in the Method section.

Materials and methods

Measurement of UV radiation

The UV measurements were conducted in the megacity of Hong Kong (22°N, 114°E) during summer months in 2015 under clear-sky/near clear-sky conditions with very low aerosol loadings (aerosol optical depth, AOD $\sim$ 0.2; except the study on aerosol effects mentioned later). Four urban sites (i.e., Sites 1–4 mentioned in the Results and Discussion section) surrounded by high-rise buildings with more than 40 storeys were selected to study the effects of solar UV reduction due to the building obstruction. One of the sites (i.e., Site 2) was selected to study the effects of building reflection at the pedestrian level since the surrounding skyscrapers were built with reflective curtain walls. An additional site at the center of an urban area was selected to study the aerosol effects on the reduction in the solar UV radiation. For Site 1, the measurement locations were between the high-rise buildings and coastline. For Sites 2 and 4, the locations were surrounded by the high-rise buildings. For Site 3, the measurements were undertaken between the high-rise buildings and a relatively large playground. All sites were paved with concrete. The geographical and architectural information of each site were provided in the Supplementary Information. The sampling height was 1.5 m above the pedestrian level. For the study on the building obstruction effects, two sampling locations (Positions A and B) were selected to capture the local variability of the total UV exposure rates due to the complex urban building obstruction effects, with their separation distances ranging between 20 and 50 m. These locations were also at least 15 m away from any building wall and without any immediate obstacles (such as trees and fences). Only one meter was available for our measurements so truly simultaneous measurements at positions A and B were not possible. Due to this limitation, alternate and sequential measurements were made to obtain at least three sets of measurements for each position, i.e., ABABAB. Fortunately, positions A and B were close to each other, so the time gap between the sequential measurements was less than 30 s. Moreover, effectively constant readings were obtained during our cloudless measurement periods. These could help make the measurements "pseudo" simultaneous. The daytime total UV exposure rates were measured six times per day. For the study on aerosol effects, only one sampling location 3 m away from the nearest building wall was adopted. All the UV exposure rates were measured using the Solarmeter standing on a horizontal surface, with the sensor probe pointing perpendicularly upwards at all time. Such a protocol was also used in other similar studies [11,23,24].

The Solarmeter Model 5.0 Total UV (UVA + UVB) Meter (hereafter referred to as "the meter") from Solartech Inc. (MI, USA) (http://www.solarmeter.com/model5.html) was employed to measure the total UV (UVA + UVB) exposure rate (Wm^{-2}). The meter was used by Chun and Yu [17] with discussion related to the calibration. The meter was calibrated on 12 March 2014 through the transfer of readings from a Standard Meter (Serial No. 03278) simultaneously and equidistant from a solar UV light source, while the Standard Meter had been calibrated according to NIST standards. According to the certificate of traceability, the accuracy of readings was ±5%. A pilot field measurement study using the meter was performed at the roof top of a building at City University of Hong Kong, which did not have nearby obstacles. The field performance of the meter was compared with the routine UV measurements by the HKO, which would be discussed in the Results and Discussion section.

Modelling of UV radiation in urban environment

A radiative transfer model, NCAR Tropospheric Ultraviolet and Visible Radiation (TUV) Model [25], was employed to simulate the UV radiation in unobstructed environments. It calculated the (direct and diffuse) UV-A and UV-B exposure rates, and the effects from aerosols were taken into consideration. The TUV model has been widely used in various UV studies [20,21,25] and other related solar radiation studies [26,27]. It was run on days which matched the mentioned sampling days for comparison. All other model setting and evaluation with observations were detailed by Wai et al. [21]. Briefly, the UV radiation was calculated using 8-stream discrete ordinate approach [28]. The model default aerosol profile by Elterman (1968) [29] was adopted for all simulations. The AOD at 388 nm and column ozone were obtained by the NASA's Ozone Monitoring Instrument (OMI) Level 3 observations. The AOD value of 0.2 was used for the "clear-sky" condition unless otherwise specified. The surface albedo was set to 0.1. The aerosol single scattering albedo was set as the model default (0.99). The reductions in solar radiation by building obstruction effects were simulated by a widely used commercial software, Autodesk Ecotect, which was also described by Wai et al. [21] (and reference therein). As in other studies, building reflections were excluded (see Erdélyi et al. [30] and references therein). The direct and diffuse UV-A and UV-B radiation inputs for the 3D Ecotect model were provided by the TUV model. Specific building configurations and the surrounding environment being simulated in the 3D Ecotect model would be discussed in the Results and Discussion sections. The 3D building configurations were obtained from scaled maps and site visits. The combined TUV and Ecotect models are referred to as the coupled model in the present work.

Results and discussion

Correlation between UV measurements at the University campus and HKO

Fig. 1 shows the very strong correlation (r^2=0.98, n = 21) between UVA measurements at HKO and total UV measurements at the CityU campus, which the latter representing the unobstructed total UV exposure rate. Comparing with the HKO's measurements, the results of the university campus were always higher, which was attributed to the contribution of UVB radiation. The results also demonstrated that our meter performed well. Furthermore, the HKO's measurements could be used to derive the unobstructed total UV exposure rate as follows:

$$\text{Un-obstructed total UV exposure rate}(Wm^{-2}) = 1.131 \times [\text{HKO's UVA exposure rate}(Wm^{-2})] - 1.659 \quad (1)$$

All the un-obstructed UV radiation levels reported here were derived by this method.

Building obstruction effects on solar total UV exposure rates

Fig. 2 shows the daytime variation of the measured total solar UV exposure rates for the four urban sites. The measurement sites were described in the Methods section. The un-obstructed total solar UV exposure rates derived as above were also included. The

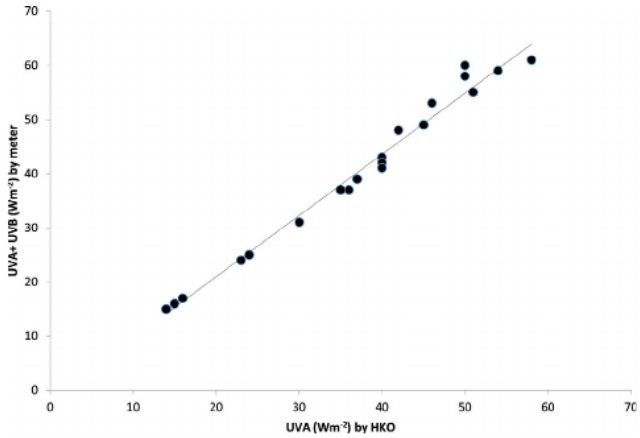

Fig. 1. The relationship between the HKO's UVA measurements and UVA + UVB measurements made using the meter at the roof top of a building in the campus of the City University of Hong Kong (solid circles).

average reduction in the total solar UV exposure rate during daytime due to the building obstruction effects at Positions A and B are summarized in Table 1. Based on the measurement results shown in Fig. 2, temporal differences for the building obstruction effects occurred for each sampling position and each site, depending on the building settings at each site. For instance, only Position B at Site 3 (Fig. 2c) was in the shadow of high-rise buildings at 13:30 local time but both Positions A and B were in the shadow at 15:30. The obstruction effects reached their minima at noon when the sun was overhead. That is, the buildings did not block the line of sight between the Solarmeter (or the receptor) and the sun. However, the maximum total solar UV exposure rates at the pedestrian level were less than the un-obstructed exposure rates for all sites at any time. For instance, Position A of Site 4 located in an open recreational area of 0.7 hectare, which was surrounded by 20- to 40-storey high-rise residential buildings, received 80% of the un-obstructed exposure rate at noon (Fig. 2d). The UV exposure rates were dependent on direct and diffuse components of the solar radiation, as well as reflection from other sources. The UV reduction could only be due to the reduction

Table 1
Measured reduction in the total UV exposure rates due to building obstruction effects in different urban site environments.

Location	Sampling date	Percent of un-obstructed total solar exposure rate	
		Position A	Position B
Site 1	3 August 2015	65 (40)	85 (135)
Site 2	4 August 2015	76 (75)	69 (75)
Site 3	31 July 2015	68 (30)	55 (25)
Site 4	19 August 2015	55 (30)	27 (20)

Value in brackets indicated the distance (m) from the nearest high-rise building.

of the diffuse component at noon. Such component of radiation received at a receptor point is thought to be the sum of radiation scattered/emitted from all small segments of the sky dome. The distant tall buildings could reduce the diffuse solar radiation in the urban area. Therefore, even without using the Solarmeter measurements, it could be concluded that the reduction in the diffuse solar radiation in the urban environment was due to the obstruction effects of distant buildings, no matter whether the direct component was obstructed or not. The maximum reduction in the total solar exposure rate obtained from the measurement here was for Site 4 (12% of un-obstructed exposure). Due to the complex building obstruction effects in urban environments, the local variability of the total solar UV exposure rates at the pedestrian level was noticeable (Table 1) when compared with the results at Positions A and B. Despite this, the exposure rate tended to decrease when moving towards the high-rise buildings based on the results at all sampling sites. The findings of (1) less exposure in urban environment compared with the un-obstructed UV radiation; (2) large reduction of solar total UV exposure rate for Site 4 (12% of un-obstructed exposure at maximum) by measurement; and (3) exposure rate decrease when moving towards buildings supported the coupled model predictions of similar situations reported in Wai et al. [21]. The finding of (2) was consistent with those in an Australian megacity [11], which reported an average of 25% of un-obstructed total UV exposure remained at urban sites surrounded by tall buildings. Similar studies are rarely available in the literature and it is clear that they are required in future due to the important health implications.

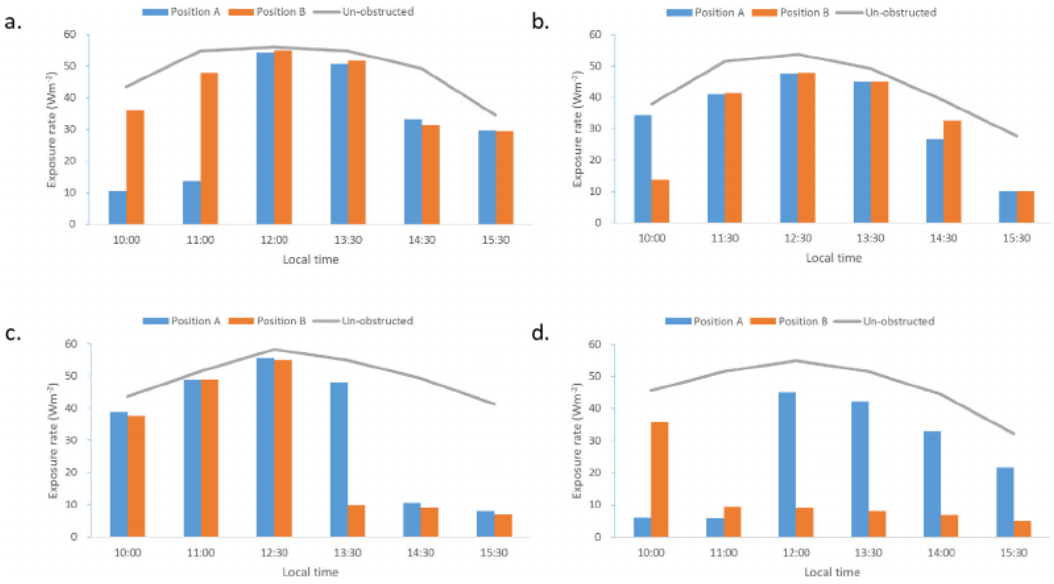

Fig. 2. Daytime variation of the total UV exposure rates at Positions A and B at the four urban sites (a) Site 1; (b) Site 2; (c) Site 3; and (d) Site 4. The un-obstructed exposure rates were also included.

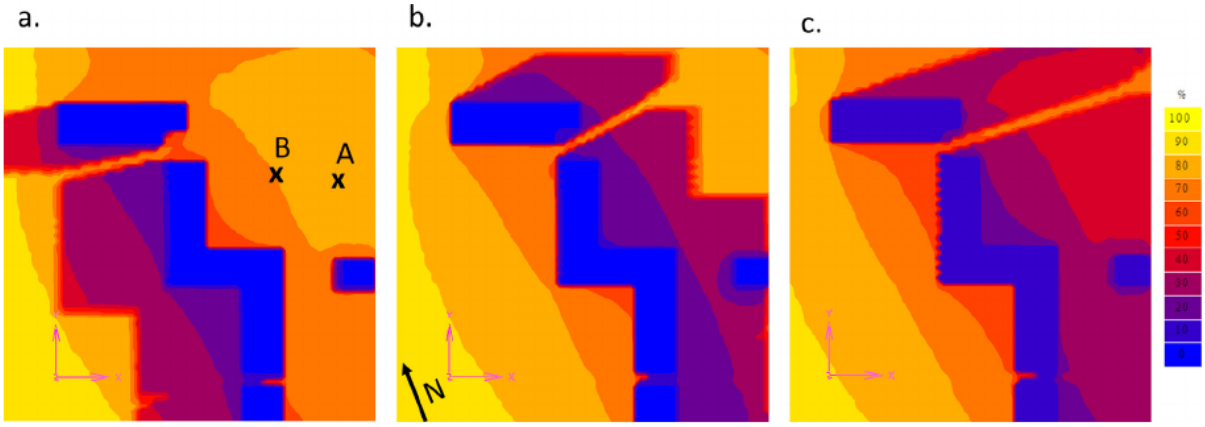

Fig. 3. Distribution of percentage of un-obstructed total UV exposure within a high-rising building environment at (a) 11:00, (b) 13:30 and (c) 15:30 local time for Site 3. Sampling positions A and B were also shown.

Table 2
Comparison between predicted and measured reduction of the total UV exposure rates due to building obstruction effects at Site 3.

Timing	Percent of un-obstructed total solar exposure rate			
	Position A		Position B	
	Predicted	Measured	Predicted	Measured
11:00	86	95 ± 13	80	95 ± 13
13:30	83	87 ± 12	25	18 ± 2
15:30	35	19 ± 3	29	17 ± 2

*Uncertainties represent 95% confidence intervals.

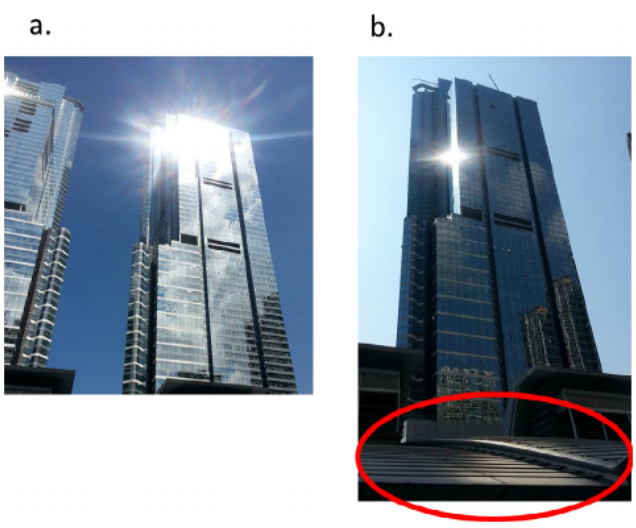

Fig. 4. (a) Solar reflection from the curtain wall of a skyscraper; and (b) a "hotspot" due to the solar reflection at ground level and the surrounding area in the building shadow (red-circled). (For interpretation of the references to colour in this figure legend, the reader is referred to the web version of this article.)

To evaluate the performance of the coupled model using the measurements mentioned in the Methods section, the model was used to simulate the reduction in the solar exposure rate at Site 3 at 11:00, 13:30 and 15:30 local time (Fig. 3 a-c). Site 3 consisted of 40-storey residential buildings (in blue near the middle of the figure). The model predictions agreed qualitatively with the measured reduction pattern for total UV radiation at Positions A and B, i.e., similar reduction in total solar exposure rates at 11:00 and 15:30 (Fig. 3a and c). The model also captured the large gradient of reduction in the UV radiation in Fig. 3b (Position B was in the building shadow but Position A was not). Table 2 showed a comparison between the predicted and measured reduction of solar exposure rates, which demonstrated reasonably good performance of the coupled model in predicting the solar exposure reduction due to building obstruction effects. The minor discrepancies between the predicted and measured reduction were due to the simplifications made in the shape of the high-rise buildings and due to the uncertainty in mimicking the complex hilly terrain (to the far east of the buildings, not shown in Fig. 3) in the model. Therefore, the balance between the model simplifications and performance should be taken into consideration for wide applications (e.g., as a tool for sustainable urban design) in future. Fig. 3a-3c also demonstrated a complex UV distribution at the pedestrian

Table 3
Exposure rate at a hotspot (in terms of percent of un-obstructed exposure rate) and the percentage enhancement on the un-obstructed exposure rate due to the presence of the hotspot.

Measurement	Sampling Date	Percent of un-obstructed total solar exposure rate		Magnitude of reflected beam relative to un-obstructed exposure rate (%)
		Hotspot inside building shadow	inside building shadow	
Set 1, morning	14 July 2015	51	28	23
Set 2, morning	4 August 2015	38	22	16
Set 3, afternoon	4 August 2015	47	36	11

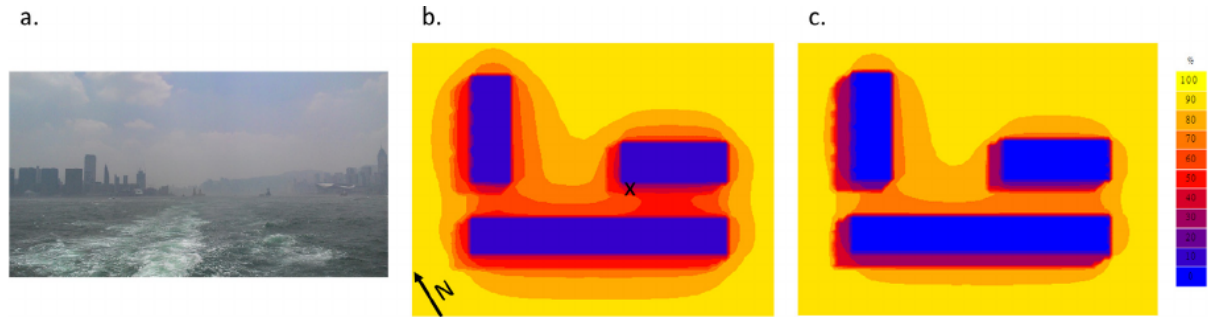

Fig. 5. (a) A snapshot of the hazy sky of the study area during an aerosol episode due to the inflow of continental pollution and stagnant air; (b) Modelled UV A + B distribution in building environment for AOD = 0.8; (c) same as (b) but AOD = 0.2. The measurement site is marked with "x".

level in the urban high-rising building environment, with a large local variability in the solar UV exposure rates within the ~4 hectare area. Furthermore, a smaller gradient of reduction in the solar exposure rate was found in the late afternoon relative to noon time.

Reflection from curtain walls on buildings

As mentioned in the Introduction, it is common in urban areas that UV distributions at the ground level are influenced by reflection of solar UV due to building wall curtains. At Site 2, we quantified the phenomenon. Fig. 4a shows strong solar reflection from the curtain wall of a skyscraper. The reflected solar beam caused a "hotspot" of light at the ground level, which was easily detected especially when the hotspot was overlaid with the building shadow area (Fig. 4b). We measured the UV enhancement of the hotspot inside the building shadow in an outdoor recreational area which was surrounded by several skyscrapers with more than 40 storeys (i.e., at Site 2). Three sets of measurements were made in the morning and afternoon to study the "hotspot" due to the curtain wall reflections from different skyscrapers (Table 3). The results showed that the UV exposure rate at the hotspot reached about twice that in the building shadow at maximum. The magnitude of the reflected beam (i.e., exposure $\text{rate}_{\text{hotspot}}$ – exposure $\text{rate}_{\text{shadow}}$, the 5th column in Table 3) relative to the unobstructed exposure rate was 23% at the maximum. It is remarked here that curtain-wall reflection occurred not only within the building shadow but also outside the shadow.

Curtain walls with reflective materials are commonly used in megacities nowadays. Our findings highlighted the considerable enhancement of UV radiation at the ground level of large parks and urban outdoor recreational areas affected by a number of high-rise buildings with reflective curtain walls, which was a common urban setting around the world. In the parks and urban outdoor recreational areas, people stayed for longer periods of time. The reflected solar beam could lead to additional UV exposure especially when the reflected beam was superimposed to the direct and obstructed diffuse solar beam. The results pointed to some improper building design which led to additional harmful effects of solar UV radiation on the environment [22].

Aerosol effects on UV distribution in urban building environment – A case study

Since the urban area is sometimes influenced by heavy aerosol loadings as mentioned, which would affect the ground-level UV distributions, we carried out measurements and conducted model evaluation during an aerosol episode to study the effects. The modelling effort was a good demonstration on how interactions among interfering factors should be considered. On 10 and 11 July 2015, a tropical cyclone was located in the southern edge of East China Sea. Its associated cyclonic flow brought polluted continental air to our studied area [14,15]. On the following day, high aerosol loadings (Fig. 5a) were maintained here due to stagnant air conditions. The aerosol episode provided an excellent opportunity to study the aerosol effects on UV distribution in the urban building environment and to evaluate the relevant model prediction. We measured the UV exposure rates in an urban environment during the time period 10:00–11:00, 12 July, and compared these with the coupled model predictions.

To simplify the case, the coupled model was set up in such a way that it included buildings (6–8 storeys) immediately surrounding the measurement site only since these buildings had dominated effects on the reduction in the UV exposure rates at the surface level (Fig. 5b). An aerosol optical depth (AOD) of 0.8 was adopted in the radiative transfer model to represent the heavy aerosol loadings[19] during the measurement period. While the predicted and measured results were comparable, the measured 31% of un-obstructed exposure rate on average was lower than the model prediction of 41% (Fig. 5b), since in reality the UV was also reduced by the buildings included in the model, although the obstruction effects were minor.

We also performed model prediction for a case without aerosol episodes (i.e., a "clear-sky case", using AOD = 0.2 with other model settings unchanged, Fig. 5c) as a reference for comparison with the prediction for the episode case. With respect to the predicted unobstructed exposure rate of 43 Wm^{-2} during the measurement period for the episode case, a stronger exposure rate of 50 Wm^{-2} was predicted for the clear-sky case. Furthermore, less pronounced spatial extents for the UV reduction due to the building obstruction effects but larger gradient of reduction were found for the clear-sky case (Fig. 5b and c), which were attributed to the lesser aerosol scattering. The predicted unobstructed exposure rate was highly comparable to the measured value of 42 Wm^{-2}. The aerosol effect on the urban UV exposure is an important topic to study since heavy aerosol ($PM_{2.5}$) loadings are concerns in many countries. More extensive works are pertinent in the future.

Concluding remarks

We measured the variations of total solar UV (UVA + UVB) exposure rates in a sub-tropical megacity which was featured with high-rising buildings located in close proximity and with curtain wall facades. Our study also included the measurements of aerosol effects on solar UV variations in the urban building environment during an aerosol episode. By measurements, large reduction in the solar total UV exposure rate down to 12% of un-obstructed exposure rate due to the building obstruction effects was found. While the reduction in the solar UV radiation for various complicated urban building environmental settings had been simulated

[22], we performed model evaluations in this study. It is essential to have well-evaluated model(s) of this kind, which is rarely available at the moment, to predict the modification of the unobstructed solar UV radiation in urban environments. The model (s) is of importance in the sustainable urban planning design to balance both the development plan for high-rise buildings and the right to enjoy adequate solar radiation in urban environments. This kind of study for different areas around the world is recommended in future with a view to improve the urban sustainability.

Acknowledgement

This work was supported by a General Research Fund CityU 125013 from the Research Grants Council of the Hong Kong SAR.

Appendix A. Supplementary data

Supplementary data associated with this article can be found, in the online version, at http://dx.doi.org/10.1016/j.rinp.2017.07.055.

References

[1] IARC. Vitamin D and Cancer Vol. 5. IARC Working Group Reports. International Agency for Research on Cancer; 2008.
[2] Holick MF. Sunlight and vitamin D for bone health and prevention of autoimmune diseases, cancers, and cardiovascular disease. Am J Clin Nutr 2004;80:1678S–88S.
[3] MacLaughlin JA, Anderson RR, Holick MF. Spectral character of sunlight modulates photosynthesis of previtamin D3 and its photoisomers in human skin. Science 1982;216:1001–3.
[4] Seckmeyer G, Schrempf M, Wieczorek A, Riechelmann S, Graw K, Seckmeyer S, et al. A novel method to calculate solar UV exposure relevant to vitamin D production in humans. Photochem Photobiol 2013;89:974–83.
[5] Halliday GM, Byrne SN, Damian DL. Ultraviolet A radiation: its role in immunosuppression and carcinogenesis. Semin Cutan Med Surg 2011;30:214–21.
[6] Mac-Mary S, Sainthillier JM, Jeudy A, Sladen C, Williams C, Bell M, et al. Assessment of cumulative exposure to UVA through the study of asymmetrical facial skin aging. Clin Interventions Aging 2010;5:277–84.
[7] Lazovich D, Vogel RI, Berwick M, Weinstock MA, Anderson KE, Warshaw EM. Indoor tanning and risk of melanoma: a case-control study in a highly exposed population. CancerEpidemiol Biomarkers Prev 2010;19:1557–68.
[8] Bernhard G, Mayer B, Seckmeyer G, Moise A. Measurements of spectral solar UV irradiance in tropical-Australia. J Geophys Res 1997;102:8719–30.
[9] Lam KS, Ding A, Chan LY, Wang T, Wang TJ. Ground-based measurements of total ozone and UV radiation by the Brewer spectrophotometer #115 at Hong Kong. Atmos Environ 2002;36:2003–12.
[10] Kim J, Cho H, Mok J, Yoo HD, Cho N. Effects of ozone and aerosol on surface UV radiation variability. J Photoch Photobio B 2013;119:46–51.
[11] McKinley A, Janda M, Auster J, Kimlin M. In vitro model of vitamin D synthesis by UV radiation in an Australian urban environment. Photochem Photobiol 2011;87:447–51.
[12] Soontrapa S, Chailurkit LO. Difference in serumcalcidiol and parathyroid hormone levels between elderly urban vssuburban women. J Med Assoc Thai 2005;88(Suppl. 5):S17–20.
[13] Goswami R, Kochupillai N, Gupta N, Goswami D, Singhand N, Dudha A. Presence of 25(OH) D deficiency in a ruralNorth Indian village despite abundant sunshine. J Assoc Physi-cians India 2008;56:755–7.
[14] Wai KM, Tanner PA. Relationship between ionic composition in PM_{10} and the synoptic-scale and mesoscale weather conditions in a south China coastal city: A 4-year study. J Geophys Res 2005;110:D18210.
[15] Wai KM, Tanner PA. Extreme particulate levels at a western Pacific coastal city: The influence of meteorological factors and the contribution of long-range transport. J Atmos Chem 2005;50:103–20.
[16] Dahlback A. Global monitoring of atmospheric ozone and solar UV radiation. In: Bjertness E, editor. Solar Radiation and Human Health. Oslo: The Norwegian Academy of Science and Letters; 2008.
[17] Chun SL, Yu PK. Calibration of EBT3 radiochromic film for measuring solar ultraviolet radiation. Rev Sci Instrum 2014;85:103–6.
[18] Butson M, Cheung T, Yu P, Abbati D, Greenoak G. Ultraviolet radiation dosimetry with radiochromic film. Phys Med Biol 2000;45:1863–8.
[19] Sabziparvar AA, Shine KP, de Forster PM. A model-derived global climatology of UV irradiance at the Earth's surface. Photochem Photobiol 1999;69:193–202.
[20] Micheletti MI, Piacentini RD. Solar UVB and Plant Damage Irradiances for Different Argentinean Regions. Photochem Photobiol 2002;76:294–300.
[21] Wai KM, Yu PKN, Lam KS. Reduction of solar UV radiation due to urban high-rise buildings – a coupled modelling study. PLoS One 2015;10:e0135562.
[22] National Geography. How Sunlight Reflected Off a Building Can Melt Objects. 2013; Available: http://news.nationalgeographic.com/news/2013/09/130904-walkie-talkie-building-london-melts-sunlight-physics-science/.
[23] Ashie Y. Study on the characteristics of solar radiation in the geometrically complex urban spaces by using a spectroradiometer. The 2nd International Conference on Countermeasures to Urban Heat Islands. Lawrence Berkeley National Laboratory, Berkeley, California. 2009; Available: http://heatisland2009.lbl.gov/docs/210900-ashie-doc.pdf.
[24] Correa MP, Ceballos JC. UVB surface albedo measurements using biometers. Rev. Bras. Geof. 2008; 26: 411-416; Available: http://www.scielo.br/scielo.php?script=sci_arttext&pid=S0102-261X2008000400002.
[25] Madronich S, McKenzie RL, Björn LO, Caldwell MM. Changes in biologically active ultraviolet radiation reaching the Earth's surface. J Photoch Photobio B 1998;46:5–19.
[26] Greenwald R, Bergin MH, Xu J, Cohan D, Hoogenboom G, Chameides WL. The influence of aerosols on crop production: a study using the CERES crop model. Agr Syst 2006;89:390–413.
[27] Wai KM, Tanner PA. Variations of aerosol properties due to regional source contributions and impacts on ozone levels: a study in a south China city. Environ Chem 2010;7:359–69.
[28] Stamnes K, Tsay SC, Wiscombe W, Jayaweera K. Numerically stable algorithm for discrete-ordinate method radiative transfer in multiple scattering and emitting layered media. Appl Opt 1998;27:2502–9.
[29] Elterman L. UV, visible, and IR attenuation for altitudes to 50 km. Air Force Cambridge Research Laboratories, Environmental Research Papers 285, AFCRL-68-0153. 1968; Available: http:// www.dtic.mil/cgi-bin/GetTRDoc?AD=AD0671933.
[30] Erdélyi R, Wang Y, Guo W, Hanna E, Colantuono G. Three-dimensional SOlar RAdiation Model (SORAM) and its application to 3-D urban planning. Sol Energy 2014;101:63–73.